OZONESONDE QUALITY ASSURANCE

The JOSIE–SHADOZ (2017) Experience

Anne M. Thompson, Herman G. J. Smit, Jacquelyn C. Witte, Ryan M. Stauffer, Bryan J. Johnson, Gary Morris, Peter von der Gathen, Roeland Van Malderen, Jonathan Davies, Ankie Piters, Marc Allaart, Françoise Posny, Rigel Kivi, Patrick Cullis, Nguyen Thi Hoang Anh, Ernesto Corrales, Tshidi Machinini, Francisco R. da Silva, George Paiman, Kennedy Thiong'o, Zamuna Zainal, George B. Brothers, Katherine R. Wolff, Tatsumi Nakano, Rene Stübi, Gonzague Romanens, Gert J. R. Coetzee, Jorge A. Diaz, Sukarni Mitro, Maznorizan Mohamad, and Shin-Ya Ogino

As a backbone for satellite algorithms and monitoring stratospheric ozone recovery, ozonesondes require regular evaluation, here performed by operators of the tropical SHADOZ network.

The periodic ozone assessments sponsored by Albritton et al. (1991, 1995), Ajavon et al. (2011, 2015), and related studies have long recognized the role of ozonesondes in the suite of global observations because sondes are the only technique practical for in situ monitoring of profiles. The sonde instrument is easy to deploy in remote locations and is relatively inexpensive. Sondes operate in both the troposphere and stratosphere (see sidebar "Ozone in the Earth's atmosphere") and in clouds, precipitation, and periods of darkness. Most important, as they ascend, ozonesondes measure ozone with an effective resolution of 100–150 m, far better than satellites. Indeed, sondes, like the ground-based networks of lidar, Dobson, and other spectrometers, constitute an essential component of satellite calibration and cross calibration (Fishman et al. 2008; Hubert et al. 2016; Steinbrecht et al. 2017; Tarasick et al. 2018, manuscript submitted to *Elementa*). The vertical structure of ozone as measured at a typical tropical station appears in the "Ozone in the Earth's atmosphere" sidebar, along with background on ozone in the atmosphere. Although dozens of stations began launching ozonesondes in the 1970s and 1980s, the concepts of standardizing and testing instruments in a coordinated network did not evolve until the 1990s (Mohnen 1996; Melamed et al. 2015). This was the period when both JOSIE and SHADOZ began (see the appendix for a list of key acronyms used in this article).

Over 50 years of ozonesonde data taking, there have been several instrument designs. Furthermore, as instruments have changed and preparation and data-processing techniques have evolved over time, time series of data from individual stations often display discontinuities and gaps that lead to inhomogeneous data records. Thus, the reliability of ozonesonde trends was questioned in some of the earlier ozone assessments (Albritton et al. 1991, 1995; Harris et al. 1998).

Two approaches have been used to address these deficiencies. First, evaluations of ozonesonde types in a controlled laboratory environment were undertaken in the 1990s, a process that continues periodically to this day. Second, in a similar manner, by testing different sonde preparation methods and protocols for data recording and processing, a set of standard operating procedures (Smit et al. 2014) was developed through consensus with the ozonesonde research community. Finally, there are recommended methods for reprocessing long-term records compromised by inhomogeneities (Smit et al. 2012; Deshler et al. 2017).

The need to have recommended instruments and procedures for emerging WMO/GAW stations in the 1990s provided a framework for the first intercalibration and intercomparisons of existing ozonesonde types. To assess the performance of the various ozonesonde instrument types used within GAW, the ESC at the FZJ (Germany) was established as the WCCOS in 1996. The chamber enables control of pressure, temperature, and ozone concentration as it simulates flight conditions of ozone soundings up to an altitude of 35 km (Smit et al. 2000). This controlled environment and comparison of the ozonesonde profiles with an accurate UV photometer as a reference (Proffitt and McLaughlin 1983) are essential requirements for addressing instrument issues that arise from field and laboratory operations.

The initial JOSIE, performed in 1996 (JOSIE-1996; Smit and Kley 1998), was the first GAW activity directed toward implementing a global quality assurance plan for ozonesondes in routine use. By now, JOSIE experiments have provided over 20 years of ozonesonde data-quality assurance to the larger atmospheric research and remote sensing communities. JOSIE-1996 was attended by eight laboratories from seven countries representing the major types of ozonesondes: ECC sondes of two manufacturers, the Brewer–Mast sonde (BM-original), the Indian sonde (a modified BM type), and the Japanese Meisei sonde (KC79). JOSIE-1996 revealed important information not only about ozonesonde performance but also about the influence of operating procedures for sonde preparation and data correction that often varied among the participating laboratories. The succession of JOSIE campaigns (Table 1) has shown that there is an ongoing need to evaluate ozonesondes because the instruments, preparation procedures, and/or the sensing solutions are modified, often inadvertently, over time. Routine testing of newly manufactured ozonesondes on a regular basis coupled with better standardization of operating procedures help ensure more confidence in the data itself as well as trends calculated from the data.

The overall objective of WCCOS and the JOSIE series of experiments has been the establishment of a facility for ozonesonde QA that can be used by sonde manufacturers and the research community. Instrumental performance of sondes from different manufacturers is tested through comparison of profiling capabilities with a standard ozone profile that

AFFILIATIONS: Thompson—NASA Goddard Space Flight Center, Greenbelt, Maryland; Smit—Institute of Chemistry and Dynamics of the Geosphere: Troposphere, Jülich Research Centre, Jülich, Germany; Witte—NASA Goddard Space Flight Center, Greenbelt, and Science Systems and Applications Inc., Lanham, Maryland; Stauffer—NASA Goddard Space Flight Center, Greenbelt, and Universities Space Research Association, Columbia, Maryland; Johnson—Global Monitoring Division, NOAA/Earth System Research Laboratory, Boulder, Colorado; Morris—Natural Sciences, St. Edward's University, Austin, Texas; von der Gathen—Alfred Wegener Institute, Potsdam, Germany; Van Malderen—Royal Meteorological Institute of Belgium, Brussels, Belgium; Davies—Environment and Climate Change Canada, Toronto, Ontario, Canada; Piters and Allaart—Royal Dutch Meteorological Institute, de Bilt, Netherlands; Posny—Laboratoire de l'Atmosphère et des Cyclones, UMR8105, Université de la Réunion, Météo-France, CNRS, La Réunion, France; Kivi—Finnish Meteorological Institute, Sodankylä, Finland; Cullis—Global Monitoring Division, NOAA/Earth System Research Laboratory, and Cooperative Institute for Research in Environmental Sciences, Boulder, Colorado; Anh—Vietnam Meteorological Hydrological Administration, Hanoi, Vietnam; Corrales and Diaz—University of Costa Rica, San Pedro, San José, Costa Rica; Machinini and Coetzee—South African Weather Service, Pretoria, South Africa; da Silva—Laboratory of Environmental and Tropical Variables, Brazilian Institute of Space Research, Natal, Brazil; Paiman and Mitro—Meteorological Service of Suriname, Paramaribo, Suriname; Thiong'o—Kenyan Meteorological Department, Nairobi, Kenya; Zainal and Mohamad—Atmospheric Science and Cloud Seeding Division, Malaysian Meteorological Department, Petaling Jaya, Selangor, Malaysia; Brothers—CHEMAL, and NASA Wallops Flight Facility, Wallops Island, Virginia; Wolff—Science Systems and Applications Inc., Lanham, Maryland, and NASA Wallops Flight Facility, Wallops Island, Virginia; Nakano—Japan Meteorological Agency, Tokyo, Japan; Stübi and Romanens—MeteoSwiss, Payerne, Switzerland; Ogino—Department of Coupled Ocean-Atmosphere-Land Processes Research, Japan Agency for Marine-Earth Science and Technology, Yokosuka, Japan

CORRESPONDING AUTHOR: Anne M. Thompson, anne.m.thompson@nasa.gov

The abstract for this article can be found in this issue, following the table of contents.

DOI:10.1175/BAMS-D-17-0311.1

In final form 15 August 2018

simulates a typical ascent in polar, midlatitude, or tropical conditions. Regular evaluation of procedures and methods at long-term ozone sounding stations with a single ozone reference instrument ensures the traceability and consistency of the records.

Over time, the SOP have been established and updated as needed. The first major SOP documentation appeared as a WMO/GAW report (GAW 201; see Smit et al. 2014) with major contributions from prior reports and Smit et al. (2007). GAW 201 was also based on field tests of the major sonde types used in the JOSIEs through 2009. A gondola of 18 instruments was flown along with the same UV photometer used in JOSIE-2000 as reported in Deshler et al. (2008).

Table 1. JOSIE activities on ozonesonde procedures and related reports.

Campaign	Objective
JOSIE-1996 GAW Report 130	• Operating procedures • Profiling capabilities • Intercomparison sonde types (ECC, BM, Meisei)
JOSIE-1998 GAW Report 57	• Manufacturing ECC sondes (SPC, ENSCI)
JOSIE-2000 GAW Report 158 (Smit et al. 2007)	• Operating procedures • Focus on ECC sonde o Different sensing solution types o Different manufacturers (SPC, ENSCI)
BESOS-2004 (Deshler et al. 2008)	• Operating procedures under flight conditions • Focus on ECC sonde o Different sensing solution types o Different manufacturers (SPC, ENSCI)
ASOPOS 2002–12 GAW Report 201	• Define and establish SOP for ECC sondes
JOSIE-2009	• Manufacturers (SPC, ENSCI)
JOSIE-2010	• Refurbished sondes
O3S-DQA Guidelines Report 2012	• Homogenization and uncertainties
JOSIE–SHADOZ 2017	• Operating procedures • Tropical simulations • Different sensing solution types • Different manufacturers (SPC, ENSCI)

SHADOZ AND UNRESOLVED SONDE ISSUES.

SHADOZ AND UNRESOLVED SONDE ISSUES. The SHADOZ network began in 1998 as an international partnership to enhance the number of tropical ozone soundings from operational stations (Thompson et al. 2003a,b, 2004, 2007, 2011). SHADOZ uses ECC ozonesondes that, over time, have been coupled with a variety of radiosondes (Table 2). A history of ozonesonde–radiosonde pairings used at SHADOZ sites appears in archival papers (Thompson et al. 2003a,b, 2007; Witte et al. 2017). At the time SHADOZ began, all known operational stations were in the Southern Hemisphere, but gradually Northern

Table 2. SHADOZ stations operating for at least 10 years between 1998 and 2017.

Station	Lat, lon	Current ECC sensor	Current radiosonde
Pago Pago, American Samoa	14.23°S, 170.56°W	ENSCI	iMet-1
Hilo, Hawaii	19.40°N, 155.00°W	ENSCI	iMet-1
San Cristóbal, Galapagos, Ecuador	0.92°S, 89.60°W	ENSCI	Vaisala RS92
San Pedro, Costa Rica	9.94°N, 84.04°W	ENSCI	iMet-1
Paramaribo, Suriname	5.81°N, 55.21°W	SPC	Vaisala RS92
Ascension Island	7.98°S, 14.42°W	ENSCI	iMet-1
Natal, Brazil	5.42°S, 35.38°W	SPC	Lockheed-Martin-Sippican LMS6
Irene, South Africa	25.90°S, 28.22°E	SPC	Vaisala RS92
Nairobi, Kenya	1.27°S, 36.80°E	ENSCI	Vaisala RS92
La Réunion, France	21.10°S, 55.48°E	ENSCI	Modem M10
Kuala Lumpur, Malaysia	2.73°N, 101.70°E	ENSCI	GRAW DFM-09
Hanoi, Vietnam	21.02°N, 105.80°E	ENSCI	Vaisala RS92
Watukosek, Java, Indonesia	7.57°S, 112.65°E	ENSCI	—*
Suva, Fiji	18.10°S, 178.40°E	ENSCI	iMet-1

* Operated Meisei RS II-KC79D radiosonde–ozonesonde system 1992–99; Vaisala RS80 1998–2013.

OZONE IN THE EARTH'S ATMOSPHERE

The ozone molecule (O_3) plays several important roles in the Earth's atmosphere. Its absorption of radiation warms the stratosphere, leading to the temperature inversion between-the troposphere and stratosphere (Fig. SB1). The inversion is typically referred to as the tropopause, but we use the term "tropopause transition layer" to signify that the tropopause is a region (~130–70 hPa) in which a number of physical properties gradually change. Most ozone molecules (80%–90%) reside in the stratosphere, so harmful UV radiation is blocked from reaching the Earth's surface. In the free troposphere, ozone acts as a greenhouse gas and is estimated to be responsible for 1/4 to 1/3 of Earth's warming over the past 200 years. Tropospheric ozone is also a source of the OH free radical, the primary oxidant in the atmosphere, responsible for reacting with hundreds of species (Thompson 1992). Ozone at the surface is considered a pollutant, harmful to human and plant health when it exceeds 3 mPa (Fig. SB1).

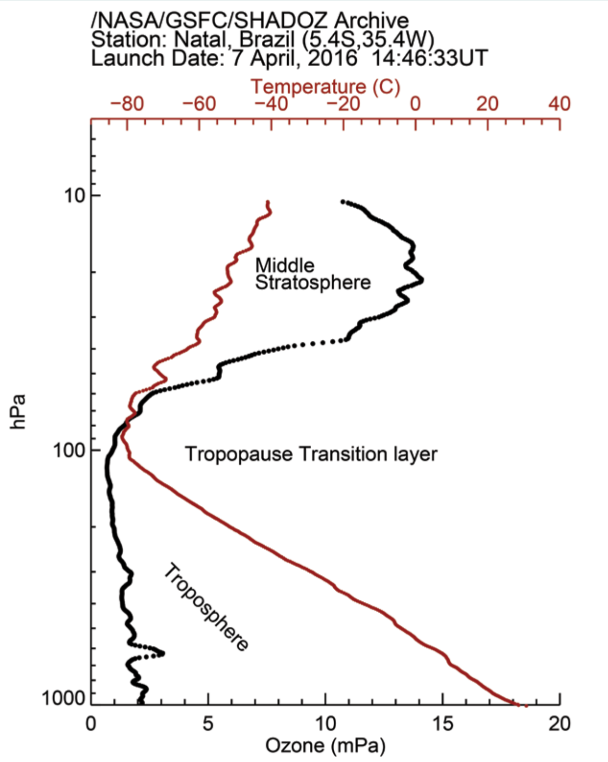

► **Fig. SB1. Ozone and temperature profiles from a typical SHADOZ sounding at Natal, Brazil, taken from the archive (https://tropo.gsfc.nasa.gov/shadoz).**

Hemisphere stations joined: Kuala Lumpur, Malaysia; Paramaribo, Suriname; San Pedro, Costa Rica; Hanoi, Vietnam; and Hilo, Hawaii. The 14 long-term stations, defined as operating at least a decade during SHADOZ, appear in Fig. 1. More than 7,000 sets of ozone and pressure–temperature–humidity profiles from SHADOZ are available online (https://tropo.gsfc.nasa.gov/shadoz).

Periodic evaluations of SHADOZ data have examined three parameters. First, TCO from the sonde, with an appropriate extrapolation above balloon burst (e.g., McPeters and Labow 2012), is compared to TCO from collocated ground-based instruments (Brewer, Dobson, SAOZ) and satellite overpasses. Second, stratospheric profiles are compared to satellite overpass ozone profiles from instruments like SAGE II (to 2005), SBUV (entire record; 1998–2016), or *Aura*'s MLS (2005–present). Third, for the tropical stations (generally within 18° latitude of the equator), stratospheric column ozone and profiles are compared. The tropical TCO is typically constant to within 3–5 DU, so measurement biases from station to station can be identified (Thompson et al. 2017).

The first three years of SHADOZ TCO compared to the EP/TOMS satellite TCO disagreed by ~8% on average, with a number of stations displaying a discrepancy of greater than 10%; the sonde TCO was usually lower than the satellite (or ground-based instrument). After the JOSIE-2000 campaign (Smit et al.

Fig. 1. Map of SHADOZ stations.

2007), in which the instruments and techniques used at all the SHADOZ stations were tested, several stations changed their sensing solution type, resulting in reduced offsets (Thompson et al. 2007). Further changes in sonde preparation procedures and subsequent reprocessing of the data, both in accordance with WMO/SPARC/IOC/NDACC guidelines (Smit et al. 2012, 2014), brought TCO for 12 of 14 stations to within 2% of TCO from three BUV-type satellites (EP/TOMS, OMI, and OMPS) operating over the 1998–2016 period (Thompson et al. 2017); the remaining two stations show TCO data averaging within 5% of the satellite TCO. These improvements derive from the application of "transfer functions" that relate a profile from each instrument–SST combination to data from the standard reference. Each profile in a time series is examined for possible correction (Witte et al. 2017, 2018).

Although the reprocessing of prior SHADOZ data has greatly reduced systematic variations in the record, JOSIE–SHADOZ was designed to address several outstanding issues. First, transfer functions determined by Deshler et al. (2017) are used to homogenize SHADOZ readings that are taken with different SST and/or instruments. This includes the 1% potassium iodide (KI), 0.1 buffer SST used at stations supported by NOAA since the mid-2000s (Sterling et al. 2018). Second, a few stations

Fig. 2. (a) Session 1 participants: 1) George Brothers (NASA WFF), 2) Kennedy Thiong'o (Kenya Meteorological Department), 3) Francisco Raimundo da Silva (INPE Natal), 4) Ernesto Corrales (University of Costa Rica), 5) Peter von der Gathen (Alfred Wegener Institute), 6) Herman Smit (FZJ), 7) Ryan Stauffer (NASA GSFC), 8) Gary Morris (St. Edward's University), 9) Gabi Nork (FZJ), 10) Anne Thompson (NASA GSFC), 11) Bryan Johnson (NOAA/ESRL), 12) Tshidi Machinini (South African Weather Service), 13) Tatsumi Nakano (Japan Meteorological Agency), and 14) Rhonie Wolff (NASA WFF). (b) Session 2 participants: 1) Gonzague Romanens (MeteoSwiss), 2) Torben Blomel (FZJ), 3) Jennifer Gläser (FZJ), 4) Nguyen Thi Hoang Anh (Vietnam Meteorological and Hydrological Administration), 5) Anne Thompson (NASA GSFC), 6) Jonathan Davies (Environment and Climate Change Canada), 7) Zamuna Zainal (Malaysian Meteorological Department), 8) Patrick Neis (FZJ), 9) Gabi Nork (FZJ), 10) Rigel Kivi (FMI), 11) Rene Stübi (MeteoSwiss), 12) Patrick Cullis (NOAA/ESRL), 13) Herman Smit (FZJ), 14) Marc Allaart (KNMI), 15) Roeland Van Malderen (KMI), 16) Jacquelyn Witte (NASA GSFC), 17) George Paiman (Meteorological Department of Suriname), 18) Andreas Petzold (FZJ), 19) Gilbert Levrat (MeteoSwiss), and 20) Françoise Posny (University of La Réunion).

in SHADOZ changed SST unintentionally and introduced discontinuities in station time series (Thompson et al. 2017; Witte et al. 2017, 2018). Finally, several stations employing a given sonde type show sharp discontinuities after 2014 that appear to originate with changes in manufacture (Sterling et al. 2018; Thompson et al. 2017).

JOSIE–SHADOZ 2017 GOALS. Similar to prior JOSIE campaigns, the major objectives of JOSIE–SHADOZ are as follows:

1) Evaluate ozonesonde instrument performance, specifically the pump and sensor as delivered by the ECC sonde manufacturer. Most of the SHADOZ stations operate with WMO-recommended solutions and preparation and calibration procedures that allow the experimenters to update the typical performance of the instruments relative to the OPM reference instrument (Proffitt and McLaughlin 1983).
2) Evaluate current preparation and operating procedures of each SHADOZ station. Unlike prior JOSIE experiments, in 2017 personnel representing the practices of all currently operating SHADOZ stations participated (Fig. 2; Tables 2 and 3; see sidebar "Capacity building during JOSIE–SHADOZ"). In most cases the operators supplied solutions as prepared at their home institution. In the first part of JOSIE-2017, the operators followed their standard practice for preconditioning sondes and for "day of flight" prior to simulation in the ESC. The goal was to understand the existing ozone profiles archived in SHADOZ by reproducing current practices, techniques, and solutions at each participating station as closely as possible.
3) Evaluate the current WMO-recommended SOP. Specific instrumental aspects examined in these tests were details of preconditioning, background current, response time, pump flow efficiency, and SST. In addition to two WMO-recommended SSTs, two alternatives, one of which is employed at several SHADOZ stations, were included in the tests.

CAPACITY BUILDING DURING JOSIE–SHADOZ

A unique feature of JOSIE–SHADOZ was that the ozonesondes were prepared by operators from organizations representing eight SHADOZ sites (see Fig. 2 showing group photos taken during both sessions in front of the WCCOS chamber). Capacity-building activities during both sessions included lectures on sonde quality assurance, the importance of metadata reporting, troubleshooting, and training with coaches from sponsoring organizations: NASA GSFC, NOAA/GMD, KNMI (Netherlands), KMI (Belgium), MeteoSwiss, Environment and Climate Change Canada, and the Finnish Meteorological Institute. Financial support for the tropical operators came from the UNEP-sponsored Vienna Convention Trust Fund, administered by WMO. Operators are essential contributors to ozonesonde quality assurance by providing detailed metadata information on each sonde launch and maintaining uniformity in their preparation and launch procedures. Bringing together SHADOZ operators for training and knowledge sharing helps to ensure that best practices are applied to operations in a consistent manner across the SHADOZ network.

Table 3. SHADOZ station operators and instruments tested in JOSIE. Participants 1–4 worked in session 1 (9–20 Oct 2017); participants 5–8 worked in session 2 (23 Oct–3 Nov 2017).

Participant No.	SST	Operator	Affiliation	Station
			Session 1	
1	1.0% full buffer	Tshidi Machinini	South African Weather Service	Irene, South Africa
2	1.0% full buffer	Francisco R. da Silva	Instituto Nacional de Pesquisas Espaciais	Natal, Brazil
3	0.5% half buffer	Kennedy Thiong'o	Kenyan Meteorological Department	Nairobi, Kenya
4	0.5% half buffer	Ernesto Corrales	University of Costa Rica	San Pedro, Costa Rica
			Session 2	
5	1.0% full buffer	George Paiman	Meteorological Service of Suriname	Paramaribo, Suriname
6	0.5% half buffer	Zamuna Zainal	Malaysian Meteorological Department	Kuala Lumpur, Malaysia
7	0.5% half buffer	Françoise Posny	Université La Réunion, Météo-France, CNRS	La Réunion, France
8	0.5% half buffer	Nguyen Thi Hoang Anh	Vietnam Meteorological and Hydrological Administration	Hanoi, Vietnam

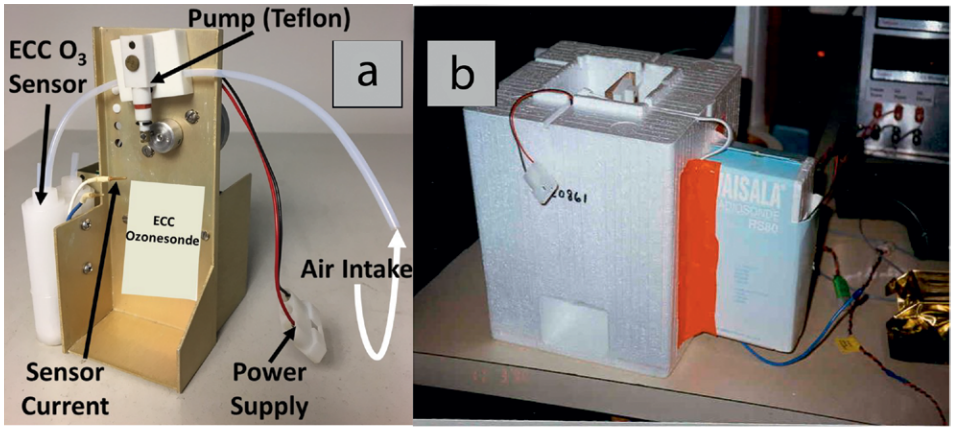

Fig. 3. (a) Schematic of an ECC in operational mode. (b) ECC instrument in Styrofoam box in which it is housed during JOSIE tests or in deployment (when launched the sensor is sealed with a Styrofoam lid). Instrument and solution type for each JOSIE–SHADOZ station appear in Tables 2 and 3, respectively.

THE OZONESONDE DESIGN. The ECC ozonesonde uses a chemical reaction measured inside a pair of cells that is displayed schematically in Fig. 3a. As the sonde rises in the atmosphere (and during the laboratory calibration phase), air is pulled through the intake tube (right side of Fig. 3a) and pushed into the cathode cell by means of a small pump. The pump maintains positive pressure as the air is sampled; the flow rate is measured during preflight calibration. The second cell (anode) is filled with a saturated version of the cathode solution and is located adjacent to the cathode, with an ion bridge separating the two cells. The reacting chemical, oxidized by the ozone molecule, is dissolved KI. The sensing solution is maintained at a neutral pH with the addition of the paired phosphates ($NaH_2PO_4 \cdot H_2O/Na_2HPO_4 \cdot 12H_2O$). The ozone partial pressure is calculated by the following equation (taken from Witte et al. 2018):

$$P_{O_3} = 4.307 \times 10^{-2} \frac{(I_M - I_B)T_P}{\Psi_P \Phi_P \eta_C},$$

where P_{O_3} = ozone partial pressure (mPa); I_M = cell current (μA); I_B = cell background current (μA); T_P = ozonesonde pump temperature (K); Ψ_P = pump flow rate (mL s^{-1}); Φ_P = pump flow efficiency (unitless); and η_C = conversion efficiency, which is generally assumed to be 1. The pump flow efficiencies Φ_P take into account the buffering of the solution, depending on the solution recipe, and mechanical degradation of the pump at low pressures (<100 hPa). The volume mixing ratio is computed from the ratio of the ozone partial pressure P_{O_3} to the ambient pressure determined from the radiosonde attached to the ozonesonde container as the two instruments ascend into the stratosphere (Fig. 3b). The typical ascent rate is 5 m s^{-1}.

From the large body of SHADOZ data as well as instruments in the field and prior laboratory intercomparisons, it is known that the two major sources of systematic error are the manufacture of the instrument and the composition of the KI and/or buffers in the SST (Smit et al. 2007). Random sources of error include operator handling and changing conditions in the station calibration unit. Calibration practices and the method of data processing can also lead to systematic differences among station profiles (Johnson et al. 2002; Deshler et al. 2008, 2017). In JOSIE–SHADOZ two types of protocols investigated these issues. The first 5 of 10 tests in each session were carried out with the operators using their own solutions and preparation technique. We refer to this as SHADOZ SOP. In the second set of tests, uniform calibration and preparation procedures were followed using JOSIE-prepared solutions, hereafter referred to as the JOSIE SOP. Unified data collection by the DAS eliminates variations due to operator data processing.

General operations during JOSIE–SHADOZ (2017). The JOSIE–SHADOZ 2017 campaign took place at the WCCOS at the FZJ in the IEK-8 in Jülich, Germany. Ozonesonde preconditioning test units and the ECC instruments were provided by FZJ from a pool of loaned supplies. Participants were split into two groups (Table 3), each of four teams operating ozonesondes of the type used in SHADOZ (Table 2). Each group participated in a 12-day intercomparison campaign. Session 1 took place from 9 to 20 October 2017; session 2 took place from 23 October through 3 November 2017. Each session consisted of 10 simulation experiments with all four participant sondes being "flown" simultaneously in the chamber (see the

DESIGN OF THE ESC, REFERENCE INSTRUMENT, DATA SYSTEM

The WCCOS, the only one of its kind, was established in the mid-1990s at FZJ to test, calibrate, and compare different types of balloon-borne ozonesondes that are used to measure the distribution of ozone in the troposphere and lower/middle stratosphere. The facility is described in more detail in Smit et al. (2000) (www.fz-juelich.de/iek/iek-8/EN/Expertise/Infrastructure/ESF/ESF_node.html).

The setup of the simulation facility (Fig. SB2a) consists of four major components:

1) Environmental simulation chamber. The ESC is a temperature-controlled vacuum chamber with a test room volume of about 500 L (80 cm × 80 cm × 80 cm). Within the ESC the pressure and temperature can be dynamically regulated, with pressures between 5 and 1,000 hPa and temperatures between 200 and 300 K, with a maximum rate of ±2 K min^{-1}. Isothermically operated, the temperature variations of the air as well as the wall inside the test room can be maintained within ±0.2 K. For more details see Smit et al. (2000).

2) OPM (ozone reference). The OPM is a fast-response dual-beam UV-absorption photometer, originally developed by Proffitt and McLaughlin (1983) for use on stratospheric balloons. The instrument was flown during BOIC missions in 1983/84 (Hilsenrath et al. 1986); it was used in the BESOS field campaign in Wyoming, in 2004 (Deshler et al. 2008). The OPM is an absolute measuring device with a 1-s response time at a sampling volume flow rate of about 8 L min^{-1}. The overall accuracy of ozone measurements made by the OPM is better than ±2% for simulated altitudes up to 25 km (pressures down to 25 hPa) and ±3.5% at 30–35-km altitude (12–5 hPa). The instrument resides in a separate vacuum vessel, which is connected to the ESC such that the UV photometer has the same pressure conditions as inside the test chamber.

3) OPS. The OPS is a gas-flow system that controls the ozone concentrations sampled by the instruments in the ESC, with a gas flow rate of 12–15 L min^{-1}. The OPS can simulate vertical ozone profiles between the surface and 35 km. The OPS can accommodate up to four ozonesondes, including the OPM (Fig. SB2b). The OPS has an option to specify ozone step functions or zero ozone to investigate the response time and background characteristics of ozonesondes.

4) DAS. The entire simulation process is automated by computer control in order to have reproducible conditions with respect to the simulated pressure, temperature, and ozone versus time and for recording and storing the large variety of parameters measured during the simulation process. A special electronic interface (JOSIE–ECC interface) couples the ECC sonde to the DAS, transmitting cathode cell current, pump temperature, pump motor current, and pump motor voltage (12 V). A small variable electrical heater (0–10 W) adjusts pump temperatures to values similar to actual flight temperatures.

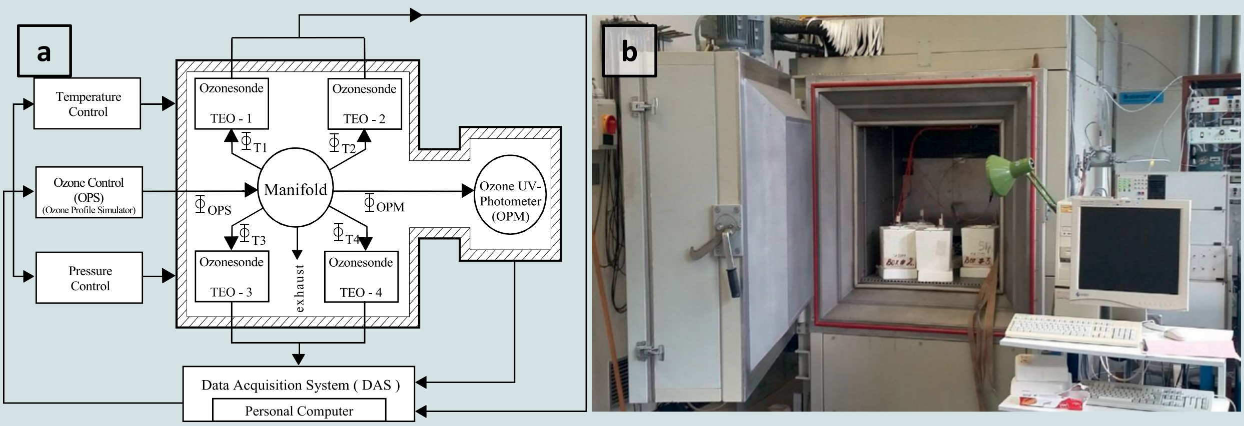

FIG. SB2. (a) Setup for the simulation of vertical ozone soundings with a schematic of the ESC, showing OPM standard reference, control systems, placement of four ozonesondes ("TEO") in the chamber, and DAS. (b) Photo of the chamber and DAS computer.

"Design of the ESC, reference instrument, data system" sidebar) to an effective altitude of ~35 km. The overall protocol for each campaign was similar, but the second session tested two "JOSIE SSTs" (Table 4). During the SHADOZ SOP (first five simulations) participants used their own zero-air filter, solutions, and preparation procedures. During the JOSIE SOPs the laboratory provided a single source of high-quality zero air, a common SST, and common operating procedures that all teams followed. Data were collected by the DAS of the WCCOS test chamber.

Because JOSIE–SHADOZ 2017 was focused on questions about SHADOZ operations, all the chamber runs simulated tropical sounding conditions

Table 4. Characteristics of JOSIE–SHADOZ 2017 simulations in the WCCOS chamber with simulation numbers listed for the two sessions. All profiles simulated with nominal 5 m s^{-1} ascent velocity. The tropopause was located at height *Z* = 18–20 km with minimum temperature around –70° to –80°C. The stratospheric profile was specified to be the same for all simulations.

Simulation No.	Troposphere profile type	Profile type index*	Specifications	ECC procedure
			Session 1	
171	Recent deep convection	1	Extremely low O_3 values nearly uniformly up to tropopause with very steep gradient into LS	Station-supplied SST and procedures
172	Maritime background	2	Low O_3 in LT, moderate O_3 in MT, extremely low O_3 in UT	Station-supplied SST and procedures
173, 174, 175, 176**	Biomass burning	3	Enhanced O_3 in LT, high O_3 in MT, low O_3 in UT	Station-supplied SST and procedures
177, 178, 179, 181	Biomass burning	3	Enhanced O_3 in LT, high O_3 in MT, low O_3 in UT	JOSIE-supplied SST and WMO procedures
180	Maritime background	2	Low O_3 in LT, moderate O_3 in MT, extremely low O_3 in UT	JOSIE-supplied SST and WMO procedures
			Session 2	
182, 183, 184,186	Biomass burning	3	Enhanced O_3 in LT, high O_3 in MT, low O_3 in UT	Station-supplied SST and procedures
185	Maritime background	2	Low O_3 in LT, moderate O_3 in MT, extremely low O_3 in UT	Station-supplied SST and procedures
187, 188, 190, 191	Biomass burning	3	Enhanced O_3 in LT, high O_3 in MT, low O_3 in UT	JOSIE-supplied SST and WMO procedures
189	Maritime background	2	Low ozone in LT, enhanced ozone in MT, and extreme low ozone in UT	JOSIE-supplied SST and WMO procedures

* In Fig. 4, 1 = blue, 2 = green, and 3 = red.

** Because of a problem with the ESC, simulation 176 recorded profiles only to 15 km.

(Fig. 4). The test profiles described in Fig. 4 and Table 4 represent three typical tropical profiles, one that is unpolluted throughout the troposphere with very low ozone near the tropopause and two with higher levels of ozone in the free troposphere and near the tropopause.

Four SST recipes were tested. All sonde data were processed by using a constant background current correction. Total ozone column normalization was not applied. The solutions, with references, follow:

1) SHADOZ 1.0. The WMO-recommended SOP (Smit et al. 2012) for use with the SPC instrument is referred to as SST 1.0% full buffer:
   Cathode: 1% KI + full buffer and KBr as described by Komhyr (1986)
   Anode: cathode solution with saturated KI
   PEF: Komhyr (1986)
2) SHADOZ 0.5. The WMO-recommended SOP (Smit et al. 2012) for use with the ENSCI instrument is referred to as SST 0.5% half buffer:
   Cathode: 0.5% KI + half of the buffer and KBr as described by Komhyr et al. (1995)
   Anode: cathode solution with saturated KI
   PEF: Komhyr et al. (1995)
3) JOSIE 1.0.1. Solution developed by NOAA for use with ENSCI sondes that has been employed at the Fiji, Samoa, Costa Rica, and Hilo stations since the late 2000s. The formulation is SST 1.0%, 1/10 buffer:
   Cathode: 1% KI + 1/10 buffer, KBr as described by Komhyr (1986)
   Anode: cathode solution with saturated KI
   PEF: new constants derived from recent pump flow measurements made by T. Nakano (2017, private communication)
4) JOSIE 2.0.1. This variation on JOSIE 1.0.1 was used to test if ozone response in the tropopause and stratosphere regions is improved by doubling the KI concentration:
   Cathode: 2% KI + 1/10 buffer; KBr as described by Komhyr (1986)

Anode: cathode solution with saturated KI

PEF: new constants derived from recent pump flow measurements made by T. Nakano (2017, personal communication)

PRELIMINARY RESULTS. Preliminary data are used to answer three questions. 1) What is the accuracy of ozone readings throughout the profile for each sonde–SST combination tested in the ESC? This is answered by comparing both the ozone partial pressure profiles measured by the sonde with the OPM and column-integrated ozone from the sondes with the OPM. For the latter, TCO and segments for troposphere, stratosphere, and the TTL in between the stratosphere and troposphere are computed. 2) How do profiles and column segments from sondes prepared with the SHADOZ SOP compare to those prepared with the JOSIE SOP? 3) What differences are observed when the same instrument type is prepared with different SST or when different instruments use the same SST? Differences are expected based on prior JOSIE results and field tests.

SHADOZ SOP. Figure 5 displays raw data from eight SHADOZ participants. The OPM measurements are represented by the black dashed lines: Fig. 5a shows the data for a simulation in session 1 (171) and Fig. 5b for a simulation in session 2 (182). The fundamental unit in the tests is lapsed time; quoted altitudes are approximate. There is some arbitrariness in designating the TTL, with the lower to middle troposphere below and the mid- to upper stratosphere above. We adopt a TTL at 2,200–3,800 s (~12–18 km) when analyzing the test results. In this region the signal-to-noise ratio is low, and therefore the uncertainty is highest (Witte et al. 2018).

In Fig. 5a the ozone partial pressures are very small throughout the "troposphere" and up to ~3,500 s or ~17.5 km. This profile simulates a near-zero-ozone tropopause, mimicking western Pacific profiles (Kley et al. 1996; Thompson et al. 2012; Rex et al. 2014; Newton et al. 2016), where SNR in ozone readings is often low. In Fig. 5b ozone partial pressure throughout the tropospheric profile is higher, representing stations influenced by biomass burning pollution in the lower to middle troposphere (Thompson et al. 1996; Jensen et al. 2012). The ozone transition near the tropopause and in the lower stratosphere in simulation 182 (Fig. 5b) lacks the sharp gradient intentionally generated in Fig. 5a. The pattern in Fig. 5b resembles that of SHADOZ stations that exhibit gradual ozone transitions in the TTL (e.g., Ascension; Natal, Brazil; and Nairobi, Kenya). Their upper-tropospheric and TTL cross sections and their contributions to the zonal wave 1 in tropical ozone are summarized in Thompson et al. (2003b, 2011, 2017).

The OPM TCO in Fig. 5a is 282 DU. The TCO from the four participants in session 1 are all higher than the OPM by 3–26 DU (up to 9%). The OPM TCO in Fig. 5b is 334 DU. The TCO from the four participants in session 2 are all equal to or higher than the OPM, with the largest offset 23 DU (7%) higher. Columns 2 and 3 in Table 5 list the corresponding TCO fractions for all eight participants relative to the OPM.

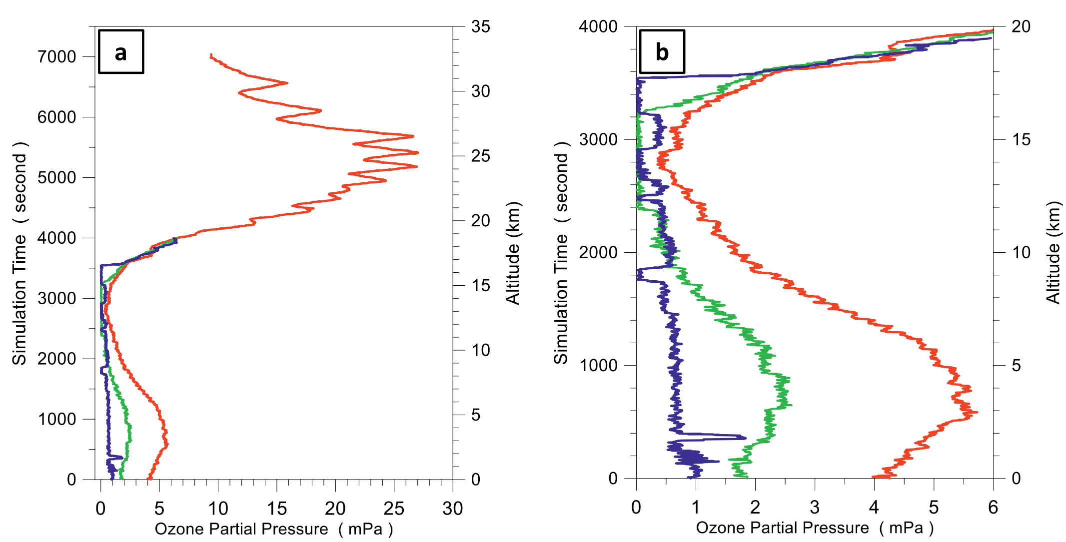

Fig. 4. Simulated ozone profiles (in partial pressure) as a function of simulation time for the troposphere and stratosphere up to (a) 33-km and (b) 20-km altitudes. Three different tropospheric ozone profiles with extremely low ozone concentrations up to the tropopause (altitude ≈ 18 km) in blue and two profiles with moderate to enhanced midtropospheric ozone values in green and red, respectively.

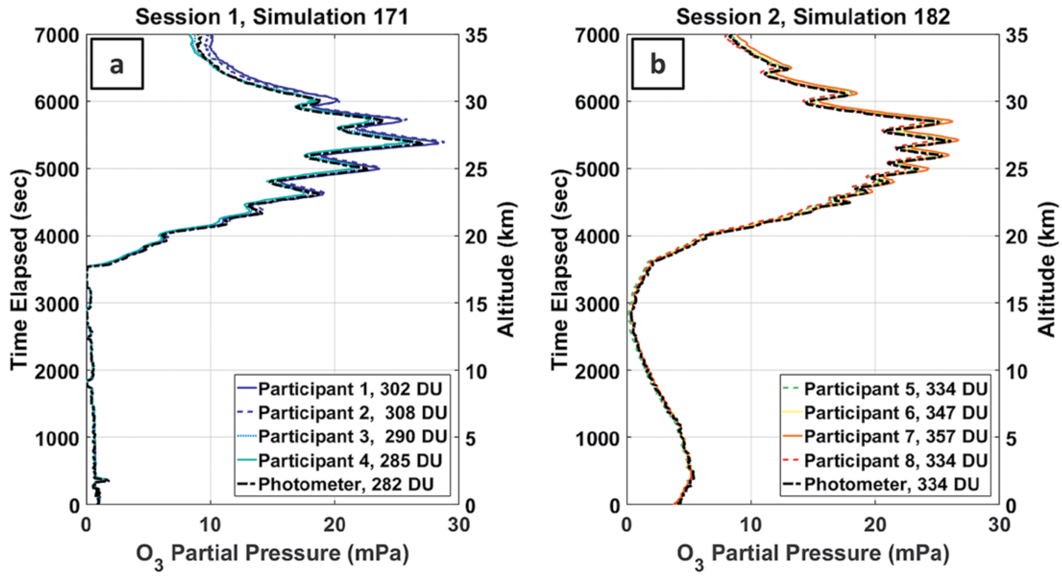

Fig. 5. Ozone "raw" profiles of typical simulations in sessions (a) 1 and (b) 2. Participants are listed in Table 3, and simulation specifications are listed in Table 4.

The means of five simulations for all eight participants, expressed as absolute and percentage differences from the OPM and based on their SHADOZ SOP are displayed in Fig. 6. The shapes of the mean profiles are broadly similar, with the sonde partial pressures (relative to the OPM; Fig. 6a) overlapping throughout the troposphere and TTL (to 3,500 s). In the stratosphere (above 4,000 s; ~20 km) differences are much larger. The fractional differences are smaller in the stratosphere (Fig. 6b), however, because the ozone partial pressure peaks at over 20 mPa (Fig. 5). The relative differences with the OPM are largely within ±10% of the OPM (zero line in Fig. 6b) throughout the lower to middle troposphere (0–2,000 s; up to 10–12 km). Around 2,000 s, there is an inflection, with the offsets all turning more negative. The largest relative differences occur within the upper troposphere (UT) and TTL (equivalent to 2,500–3,500 s; 13–18 km), exceeding 5% on average for all the stations. For participants 4 and 5 the mean relative differences exceed −20%. Witte et al. (2018) noted that SHADOZ ozone values are most uncertain in the narrow region between 15 and 17 km (~3,000–4,300 s). However, the large offsets recorded in Fig. 6b include four JOSIE tests conducted with TTL ozone equivalent to 2 DU (e.g., simulation 171; Fig. 5a), a value that applies to only ~5% of tropical SHADOZ readings.

Table 5. Total and partial column statistics from two SHADOZ simulations and means for all 10 simulations (5 each in sessions 1 and 2). All simulations use SHADOZ SOPs.

Instrument	Simulation 171 (DU)	Simulation 182 (DU)	Mean OPM/ sonde ratio: TCO	Mean OPM/ sonde ratio: tropospheric O_3 (0–15 km)	Mean OPM/ sonde ratio: TTL O_3 (12–18 km)	Mean OPM/ sonde ratio: stratospheric O_3 (15 km to end)
OPM	282	—	337 DU	47.0 DU	4.93 DU	298 DU
Participant 1	1.07	—	1.03	1.09	1.02	1.04
Participant 2	1.09	—	1.04	1.09	1.03	1.04
Participant 3	1.03	—	1.03	1.02	0.95	1.03
Participant 4	1.01	—	1.02	1.06	1.01	1.02
OPM	—	334	313 DU	41.0 DU	5.30 DU	271 DU
Participant 5	—	1.00	1.03	0.85	0.77	1.03
Participant 6	—	1.04	1.04	0.89	0.87	1.05
Participant 7	—	1.07	1.04	0.93	0.93	1.05
Participant 8	—	1.00	1.02	0.88	0.87	1.02

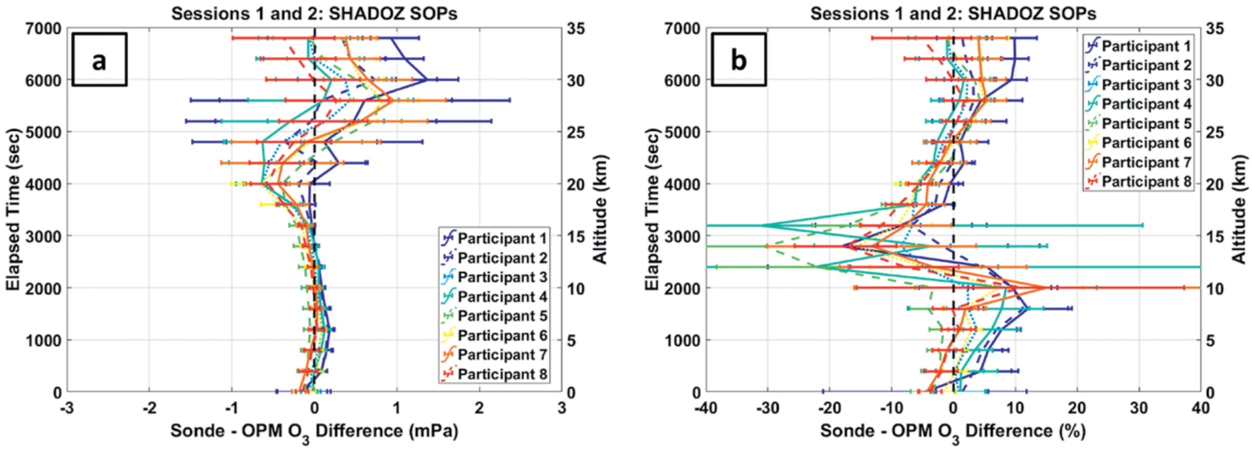

Fig. 6. (a) Participant mean profiles relative to OPM in partial pressure (mPa) and (b) percentage deviation (sonde minus OPM/OPM). Based on five simulations per participant.

Realistically, Fig. 8b in Thompson et al. (2017), based on >6,000 profiles, shows that the actual TTL ozone for 12 of 14 SHADOZ stations is 8.0 ± 1.5 DU. By 3,000 s (~15 km) the relative differences of all SHADOZ profiles with respect to the OPM start to increase. All SHADOZ profiles show excellent agreement with OPM to within ±5% at 20–25 km (critical ozone maximum). By 5,000 s (~25 km) most SHADOZ profiles exceed OPM ozone and are well aligned with one another. The range of mean deviations in the region corresponding to 20–28 km is within 10%. This tighter clustering implies good measurement precision. By ~5,500 s (27.5 km) all the SHADOZ readings are higher than the OPM. Above 30 km the agreement breaks down and there is a downturn in ozone readings relative to the OPM for most stations. Exceptions are participants 1 and 7, which display +10% and 4% deviations, respectively (Fig. 6b). The negative relative differences are not surprising. Witte et al. (2017) showed that even reprocessed SHADOZ ozonesonde data above ~30 km are highly variable and not as reliable.

How do column amounts for the SHADOZ participants compare on average to OPM ozone? Answers appear in Table 5. For the five SHADOZ simulations all of the participants record, on average, slightly more ozone than the OPM, with ratios from 1.02 to 1.04 (1.7%–4.0% more O_3). This result seems to validate the quality assurance practices of the SHADOZ stations, with seven of eight participants following the WMO-recommended instrument SST combinations and SOP (Smit et al. 2007, 2012). The segment column comparisons (columns 0–15 km, 12–18 km, and 15 km to end in Table 5) demonstrate that the good agreement between sondes and the OPM is dominated by the ozone column from 15 km to end, that is, the stratospheric portion of the profile. Because the WMO recommendations are largely based on JOSIE-2000, several follow-on laboratory tests, and the BESOS conducted in 2004, it can be inferred

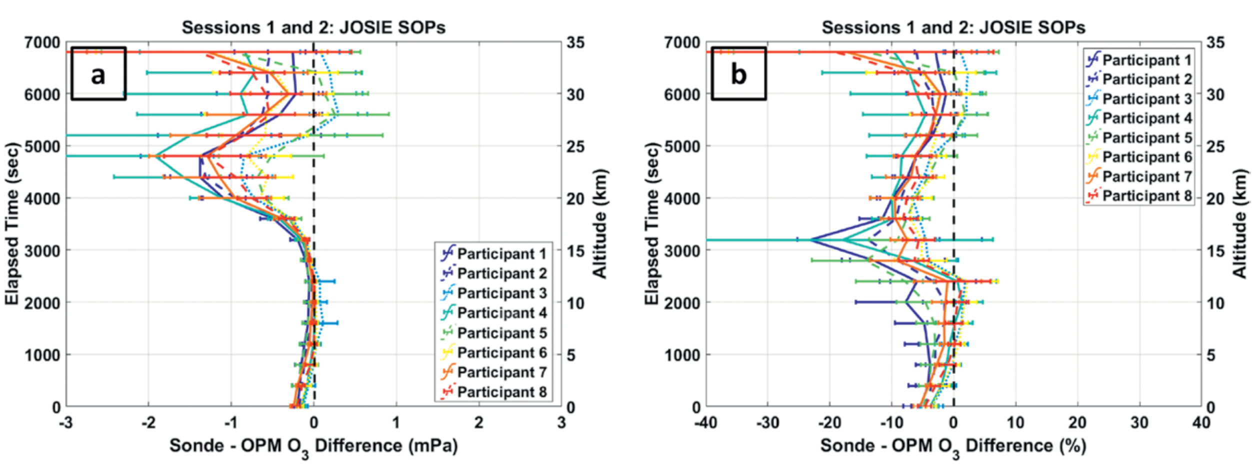

Fig. 7. As in Fig. 6, but for JOSIE SOP as described in Table 4.

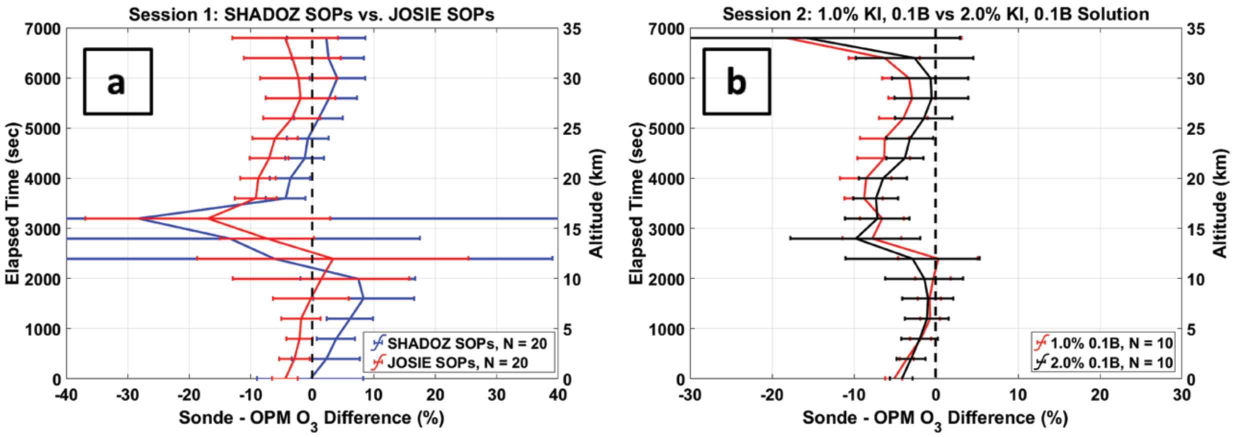

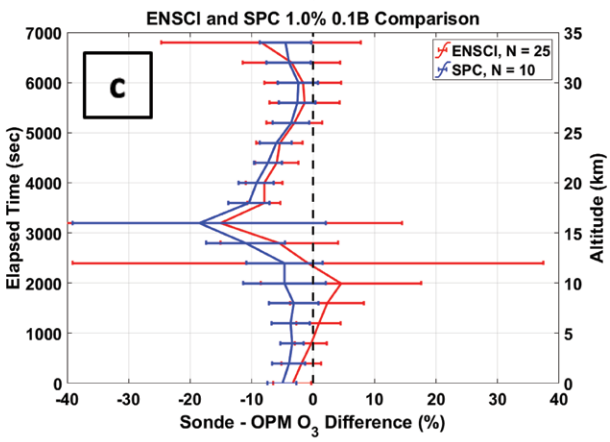

Fig. 8. (a) Session 1 SHADOZ SOP (blue) and JOSIE SOP (red) mean profiles subtracted from the OPM profile mean (% difference), (b) session 2 JOSIE 2.0.1 (black) and JOSIE 1.0.1 (red) SST profile means subtracted from the OPM, and (c) session 1 and 2 mean profiles of ENSCI OPM (red) and SPC OPM (blue) for which JOSIE 1.0.1 SST and SOP were used. One-sigma standard deviations for all panels are included.

that the WMO recommendations (Smit et al. 2012) are still valid. Agreement in the TTL (12–18-km column) averages <0.95 for half of the groups (Table 5). Because the OPM recorded only 5 DU on average in this region, the larger offsets do not detract from the good agreement overall.

JOSIE SOP. The sonde partial pressure offsets from the OPM and relative differences for the eight participants using the JOSIE 1.0.1 SST and preparation protocols appear in Figs. 7a and 7b, respectively. When these results are compared to those with the SHADOZ SOP (Fig. 6), two differences are observed. First, the divergence among stations is less with the more uniform specifications of the JOSIE SOP, especially in the midtroposphere through the TTL. This is not surprising because the use of a single SST and SOP is expected to minimize variations due to SST. The JOSIE SOP uses solutions with less buffer by a factor of 2 or 10. Thus, owing to the lower buffer the sonde responses show less of a hysteresis effect in the region with relatively fast ozone changes, resulting in increased SNR. This is particularly true in the TTL at the tropopause and just above, corresponding to the 2,500–3,500-s region in Figs. 6b and 7b. The second difference is that ozone readings throughout the profile are lower relative to the OPM with the JOSIE SOP than the SHADOZ SOP, particularly in the troposphere (Fig. 7a below 4,000 s) and even more so in the stratosphere, where the offsets are –1 to –2 mPa ozone. The result is a mean sonde TCO offset with the JOSIE SOP relative to the OPM of 0.97 (first two entries in column 3 of Table 6) compared to a mean 1.03 TCO offset with the SHADOZ SOP. Background cell currents and response times improved significantly during the JOSIE SOP in both sessions when a shared zero-air system was used.

SHADOZ–JOSIE comparisons. Figure 8a displays the average differences between the SHADOZ and JOSIE SOP profiles for session 1. For each participant in session 1, five simulations were made totaling 20 profiles of each SOP, both using the same SST. Up to 10 km the SHADOZ SOP resulted in relatively higher ozone readings; toward the TTL the JOSIE SOP resulted in higher ozone readings. The stratospheric differences, however, show the JOSIE SOP averages 3% lower TCO than the OPM while the SHADOZ SOP averages 3% higher TCO than the OPM (and stratospheric segment; Table 6). Note that the near-zero simulated ozone represents a small fraction of what is observed in SHADOZ records; thus, the large uncertainties seen in Fig. 8a represent the extrema of the dataset.

In session 2, to compensate for the reduced sensitivity of the 1.0%, 1/10 buffer SST (JOSIE 1.0.1),

Table 6. Total and partial column statistics from profile simulations, relative to OPM, categorized by SOP and sonde/solution types. In the methodology column, B stands for buffer.

Methodology	No.	Mean sonde/ OPM TCO	Mean sonde/OPM tropospheric O_3 (0–15 km)	Mean sonde/ OPM TTL O_3 (12–18 km)	Mean sonde/OPM stratospheric O_3 (20 km to end)
SHADOZ SOP	40	1.03	1.01	0.94	1.04
JOSIE SOP	40	0.97	0.99	0.94	0.97
ENSCI 1.0%, 0.1B	25	0.98	1.00	0.97	0.98
SPC 1.0%, 0.1B	10	0.97	0.96	0.90	0.98
ENSCI 0.5%, 0.5B	20	1.03	1.00	0.91	1.04
SPC 1.0%, 1.0B	15	1.03	1.01	0.95	1.04
ENSCI 2.0%, 0.1B	5	0.97	1.01	0.97	0.97
SPC 2.0%, 0.1B	5	0.97	0.94	0.90	0.96

solutions with the JOSIE SOP were prepared with twice as much KI but the same low buffer, the so-called JOSIE 2.0.1. JOSIE 1.0.1 comparisons were all made with ENSCI, whereas the JOSIE 2.0.1 referred to a combination of SPC and ENSCI. Mean profile comparisons with the different SSTs are summarized in Fig. 8b. The differences are not statistically significant throughout the troposphere or TTL, but the JOSIE 2.0.1 profile mean is closer to the OPM in the upper stratosphere (above 5,000 s). In session 2, the ratio of sonde to OPM partial column ozone above 20 km for JOSIE 1.0.1 was 0.95, while for JOSIE 2.0.1 it was 0.97. Sondes filled with both SSTs show sondes measure less ozone than the OPM in the stratosphere and are highly variable above 30 km, consistent with Fig. 7 and the Witte et al. (2018) findings.

Previous JOSIE campaigns and various field tests (especially the BESOS in 2004) noted that throughout the ozone profile when the same SST is used, the ENSCI instrument tends to measure more ozone than the SPC instrument. Of the 14 SHADOZ stations, 11 use the ENSCI instrument and 3 use the SPC type (Thompson et al. 2017; Witte et al. 2017, 2018). Figure 8c, based on the combined session simulations (JOSIE 1.0.1), shows that, also for the less buffered solutions, the ENSCI instrument measures slightly higher ozone than the SPC with the greatest discrepancies in the troposphere, consistent with previous JOSIE studies.

CONCLUSIONS.

1) All eight stations participating in JOSIE–SHADOZ 2017 measured ozone that agreed well with the OPM.
2) The slight ENSCI–SPC ozone bias (ENSCI reads higher) previously observed (Smit et al. 2007, 2012) remained in JOSIE–SHADOZ 2017.
3) JOSIE-2017 affirms the very high quality of the SHADOZ methods that use SOP and instrument–SST combinations based on earlier JOSIE campaigns and field tests as summarized in Smit et al. (2007, 2012). This is independent confirmation of the accuracy of the large SHADOZ dataset that up to now has only been compared to data from satellite and ground-based instruments (Thompson et al. 2017; Witte et al. 2017). The ozonesonde community goals of "5% accuracy and precision in TCO" have been met by SHADOZ operators engaging in collaborative ozonesonde "expert" activities since 2000. Except for the TTL, most instrument–SST combinations tested in JOSIE with SHADOZ SOP agreed within 3% of OPM in total column amount (sonde higher) and 5%–10% throughout the ozone profile. The often-large TTL ozone underestimate (>30% relative to OPM in some tests) contributes only 2%–3% of the total ozone column.
4) JOSIE tested solutions with a reduced-buffer SST, of the type used at four SHADOZ stations. As expected, agreement of sonde ozone data with the OPM in the TTL regions was improved. However, sensitivity to stratospheric ozone is reduced, so TCO from these tests averaged 3% lower than the OPM. The low bias is reduced when the KI is doubled (JOSIE 2.0.1). However, the divergence of profiles with the different SSTs is so small (~5%) that further analysis, such as taking into account individual sonde responses, is required.
5) The JOSIE SOP were as follows:
   - Lower, uniform, and better reproducible background cell currents are achieved using a high-quality no-ozone filter source or purified air.
   - The hysteresis effect ("memory" effect due to the buffering of the solution) is minimized,

which may improve the response of the sonde, particularly in the TTL where sharp ozone gradients are measured.

Because SHADOZ represents virtually all current ECC sonde practices used by the global ozone community, these findings and any SOP recommendations that ozonesonde "experts" consider in light of JOSIE-2017 should be universally valid for ECC instruments. Establishing SOP guidelines and standardization of ground equipment is essential to achieving an uncertainty less than 5% between the surface and 30-km altitude. The JOSIE–SHADOZ 2017 experience highlights the necessity of having a continuous reference calibration facility (WCCOS) operating over the past 25 years. The capacity-building exercise has empowered participants to continue working toward ensuring a high-quality standard in sonde data-taking. With well-trained and motivated operators, SOPs based on best practices, and experiments such as JOSIE–SHADOZ, our aim of an uncertainty less than 5% can be achieved.

ACKNOWLEDGMENTS. The 2017 JOSIE would not have been possible without strong support of the IEK-8 group of Forschungszentrum Jülich, including a number of technicians and Ms. Gabi Nork, who was in charge of the organizing. The United Nations Environmental Programme (S. Mylona, Nairobi) provided travel funds for SHADOZ operators. Support was also given by the Science Pump Corporation (S. Schwartz), ENSCI (J. Harnetiaux and G. Kok), and JAMSTEC (S.-Y. Ogino). SHADOZ is supported by NASA's Upper Atmosphere Research Program and Aura Validation, NOAA's Global Monitoring Division Lab (Boulder), and more than 15 organizations in SHADOZ host nations and from Japan, Switzerland, France, and the Netherlands.

APPENDIX: ACRONYMS.

ASOPOS	Assessment of SOP for Ozonesondes
BESOS	Balloon Experiment on Standards for Ozonesondes
BM	Brewer–Mast
BOIC	Balloon Ozone Intercomparison
DAS	Data acquisition system
DU	Dobson unit
ECC	Electrochemical concentration cell
ENSCI	Environmental Science Corporation
EP	Earth Probe
ESC	Environmental simulation chamber
ESRL	Earth System Research Laboratory
FMI	Finnish Meteorological Institute
FZJ	Forschungszentrum Jülich
GAW	Global Atmospheric Watch
GMD	Global Monitoring Division
GSFC	Goddard Space Flight Center
IEK-8	Institute of Energy and Climate Research: Troposphere
INPE	Instituto Nacional de Pesquisas Espaciais
IOC	International Ozone Commission
JAMSTEC	Japan Agency for Marine-Earth Science and Technology
JOSIE	Jülich Ozonesonde Intercomparison Experiment
KMI	Royal Meteorological Institute of Belgium
KNMI	Royal Netherlands Meteorological Institute
LS	Lower stratosphere
LT	Lower troposphere
MLS	Microwave Limb Sounder
MT	Midtroposphere
NDACC	Network for the Detection of Atmospheric Composition Change
O3S-DQA	Ozone Data Quality Assessment
OMI	Ozone Monitoring Instrument
OMPS	Ozone Mapping Profiler Suite
OPM	Ozone Photometer
OPS	Ozone Profile Simulator
PEF	Pump efficiency factor
QA	Quality assurance
SAOZ	Système D'Analyse par Observations Zénithales
SAGE II	Stratospheric Aerosol and Gas Experiment II
SBUV	Solar backscatter ultraviolet
SHADOZ	Southern Hemisphere Additional Ozonesondes
SNR	Signal-to-noise ratio
SOP	Standard operating procedures
SPARC	Stratospheric Processes and Their Role in Climate
SPC	Science Pump Corporation
SST	Sensing solution type
TCO	Total column ozone
TOMS	Total Ozone Mapping Spectrometer
TTL	Tropical tropopause layer (or tropopause transition layer)
UNEP	United Nations Environmental Programme
UT	Upper troposphere
WCCOS	World Calibration Centre for Ozonesondes
WFF	Wallops Flight Facility
WMO	World Meteorological Organization

REFERENCES

Albritton, D., and Coauthors, 1991: Scientific assessment of ozone depletion: 1991. Global Ozone Research and Monitoring Project Rep. 25, 326 pp.

——, and Coauthors, 1995: Scientific assessment of ozone depletion: 1994. Global Ozone Research and Monitoring Project Rep. 37, 529 pp.

Ajavon, A.-L. N., and Coauthors, 2011: Scientific assessment of ozone depletion: 2010. Global Ozone Research and Monitoring Project Rep. 52, 514 pp.

——, and Coauthors, 2015: Scientific assessment of ozone depletion: 2014. Global Ozone Research and Monitoring Project Rep. 55, 416 pp., www.esrl.noaa.gov/csd/assessments/ozone/2014/chapters/2014OzoneAssessment.pdf.

Deshler, T., and Coauthors, 2008: Atmospheric comparison of electrochemical cell ozonesondes from different manufacturers, and with different cathode solution strengths: The Balloon Experiment on Standards for Ozonesondes. *J. Geophys. Res.*, **113**, D04307, https://doi.org/10.1029/2007JD008975.

——, R. Stübi, F. J. Schmidlin, J. L. Mercer, H. G. J. Smit, B. J. Johnson, R. Kivi, and B. Nardi, 2017: Methods to homogenize electrochemical concentration cell (ECC) ozonesonde measurements across changes in sensing solution concentration or ozonesonde manufacturer. *Atmos. Meas. Tech.*, **10**, 2021–2043, https://doi.org/10.5194/amt-10-2021-2017.

Fishman, J., and Coauthors, 2008: Remote sensing of tropospheric pollution from space. *Bull. Amer. Meteor. Soc.*, **89**, 805–821, https://doi.org/10.1175/2008BAMS2526.1.

Harris, N., and Coauthors, 1998: Assessment of trends in the vertical distribution of ozone. SPARC Rep. 1/WMO Global Ozone Research and Monitoring Project Rep. 43, 290 pp., www.sparc-climate.org/fileadmin/customer/6_Publications/SPARC_reports_PDF/1_Ozone_SPARCreportNo1_May1998_redFile.pdf.

Hilsenrath, E., and Coauthors, 1986: Results from the balloon ozone intercomparison campaign (BOIC). *J. Geophys. Res.*, **91**, 13 137–13 152, https://doi.org/10.1029/JD091iD12p13137.

Hubert, D., and Coauthors, 2016: Ground-based assessment of the bias and long-term stability of 14 limb and occultation ozone profile data records. *Atmos. Meas. Tech.*, **9**, 2497–2534, https://doi.org/10.5194/amt-9-2497-2016.

Jensen, A. A., A. M. Thompson, and F. J. Schmidlin, 2012: Classification of Ascension Island and Natal ozonesondes using self-organizing maps. *J. Geophys. Res.*, **117**, D04302, https://doi.org/10.1029/2011JD016573.

Johnson, B. J., S. J. Oltmans, H. Voemel, H. G. J. Smit, T. Deshler, and C. Kroeger, 2002: ECC ozonesonde pump efficiency measurements and tests on the sensitivity to ozone of buffered and unbuffered ECC sensor cathode solutions. *J. Geophys. Res.*, **107**, 4393, https://doi.org/10.1029/2001JD000557.

Kley, D., P. J. Crutzen, H. G. J. Smit, H. Vömel, S. J. Oltmans, H. Grassl, and V. Ramanathan, 1996: Observations of near-zero ozone concentrations over the convective Pacific: Effects on air chemistry. *Science*, **274**, 230–233, https://doi.org/10.1126/science.274.5285.230.

Komhyr, W. D., 1986: Operations handbook: Ozone measurements to 40 km altitude with model 4A-ECC-ozone sondes. NOAA Tech. Memo. ERL-ARL-149, 49 pp.

——, R. A. Barnes, G. B. Brothers, J. A. Lathrop, and D. P. Opperman, 1995: Electrochemical concentration cell ozonesonde performance evaluation during STOIC 1989. *J. Geophys. Res.*, **100**, 9231–9244, https://doi.org/10.1029/94JD02175.

McPeters, R. D., and G. J. Labow, 2012: Climatology 2011: An MLS and sonde derived ozone climatology for satellite retrieval algorithms. *J. Geophys. Res.*, **117**, D10303, https://doi.org/10.1029/2011JD017006.

Melamed, M. L., P. S. Monks, A. H. Goldstein, M. G. Lawrence, and J. Jennings, 2015: The international global atmospheric chemistry (IGAC) project: Facilitating atmospheric chemistry research for 25 years. *Anthropocene*, **12**, 17–28, https://doi.org/10.1016/j.ancene.2015.10.001.

Mohnen, V., 1996: Update on IGAC's Global Tropospheric Ozone Network (GLONET) activity and the International Tropospheric Ozone Years (ITOY). *IGACtivities Newsletter*, IGAC Project Office, Boulder, CO, 4–6, www.igacproject.org/sites/default/files/2016-07/Issue_03_Jan_1996.pdf.

Newton, R., G. Vaughan, H. M. A. Ricketts, L. L. Pan, A. J. Weinheimer, and C. Chemel, 2016: Ozonesonde profiles from the West Pacific warm pool: Measurements and validation. *Atmos. Chem. Phys.*, **16**, 619–634, https://doi.org/10.5194/acp-16-619-2016.

Proffitt, M. H., and R. J. McLaughlin, 1983: Fast response dual-beam UV-absorption photometer suitable for use on stratospheric balloons. *Rev. Sci. Instrum.*, **54**, 1719–1728, https://doi.org/10.1063/1.1137316.

Rex, M., and Coauthors, 2014: A tropical West Pacific OH minimum and implications for stratospheric composition. *Atmos. Chem. Phys.*, **14**, 4827–4841, https://doi.org/10.5194/acp-14-4827-2014.

Smit, H. G. J., and D. Kley, 1998: JOSIE: The 1996 WMO international intercomparison of ozonesondes under quasi flight conditions in the environmental

simulation chamber at Jülich. WMO Global Atmosphere Watch Rep. 130, WMO/TD-926, 108 pp.
——, W. Sträter, M. Helten, and D. Kley, 2000: Environmental simulation facility to calibrate airborne ozone and humidity sensors. Jülich Research Center Rep. Jül-3796, 38 pp.
——, and Coauthors, 2007: Assessment of the performance of ECC-ozonesondes under quasi-flight conditions in the environmental simulation chamber: Insights from the Jülich Ozone Sonde Intercomparison Experiment (JOSIE). *J. Geophys. Res.*, **112**, D19306, https://doi.org/10.1029/2006JD007308.
——, S. Oltmans, T. Deshler, D. Tarasick, B. Johnson, F. Schmidlin, R. Stuebi, and J. Davies, 2012: SI2N/O3S-DQA activity: Guide lines for homogenization of ozone sonde data. SPARC–IGACO–IOC Rep., 48 pp., www-das.uwyo.edu/~deshler/NDACC_O3Sondes/O3s_DQA/O3S-DQA-Guidelines%20Homogenization-V2-19November2012.pdf.
——, and Coauthors, 2014: Quality assurance and quality control for ozonesonde measurements in GAW. World Meteorological Organization GAW Rep. 201, 94 pp., www.wmo.int/pages/prog/arep/gaw/documents/FINAL_GAW_201_Oct_2014.pdf.
Steinbrecht, W., and Coauthors, 2017: An update on ozone profile trends for the period 2000 to 2016. *Atmos. Chem. Phys.*, **17**, 10 675–10 690, https://doi.org/10.5194/acp-17-10675-2017.
Sterling, C. W., and Coauthors, 2018: Homogenizing and estimating the uncertainty in NOAA's long-term vertical ozone profile records measured with the electrochemical concentration cell ozonesonde. *Atmos. Meas. Tech.*, **11**, 3661–3687, https://doi.org/10.5194/amt-11-3661-2018.
Thompson, A. M., 1992: The oxidizing capacity of the Earth's atmosphere: Probable past and future changes. *Science*, **256**, 1157–1165, https://doi.org/10.1126/science.256.5060.1157.
——, and Coauthors, 1996: Where did tropospheric ozone over southern Africa and the tropical Atlantic come from in October 1992? Insights from TOMS, GTE TRACE A, and SAFARI 1992. *J. Geophys. Res.*, **101**, 24 251–24 278, https://doi.org/10.1029/96JD01463.
——, and Coauthors, 2003a: Southern Hemisphere Additional Ozonesondes (SHADOZ) 1998–2000 tropical ozone climatology: 1. Comparison with Total Ozone Mapping Spectrometer (TOMS) and ground-based measurements. *J. Geophys. Res.*, **108**, 8238, https://doi.org/10.1029/2001JD000967.
——, and Coauthors, 2003b: Southern Hemisphere Additional Ozonesondes (SHADOZ) 1998–2000 tropical ozone climatology: 2. Tropospheric variability and the zonal wave-one. *J. Geophys. Res.*, **108**, 8241, https://doi.org/10.1029/2002JD002241.
——, J. C. Witte, S. J. Oltmans, and F. J. Schmidlin, 2004: SHADOZ—A tropical ozonesonde–radiosonde network for the atmospheric community. *Bull. Amer. Meteor. Soc.*, **85**, 1549–1564, https://doi.org/10.1175/BAMS-85-10-1549.
——, ——, H. G. J. Smit, S. J. Oltmans, B. J. Johnson, V. W. J. H. Kirchhoff, and F. J. Schmidlin, 2007: Southern Hemisphere Additional Ozonesondes (SHADOZ) 1998–2004 tropical ozone climatology: 3. Instrumentation, station-to-station variability, and evaluation with simulated flight profiles. *J. Geophys. Res.*, **112**, D03304, https://doi.org/10.1029/2005JD007042.
——, S. J. Oltmans, D. W. Tarasick, P. von der Gathen, H. G. J. Smit, and J. C. Witte, 2011: Strategic ozone sounding networks: Review of design and accomplishments. *Atmos. Environ.*, **45**, 2145–2163, https://doi.org/10.1016/j.atmosenv.2010.05.002.
——, and Coauthors, 2012: Southern Hemisphere Additional Ozonesondes (SHADOZ) ozone climatology: Tropospheric and tropical tropopause layer (TTL) profiles with comparisons to OMI-based ozone products. *J. Geophys. Res.*, **117**, D23301, https://doi.org/10.1029/2011JD016911.
——, and Coauthors, 2017: First reprocessing of Southern Hemisphere Additional Ozonesondes (SHADOZ) ozone profiles (1998–2016): 2. Comparisons with satellites and ground-based instruments. *J. Geophys. Res. Atmos.*, **122**, 13 000–13 025, https://doi.org/10.1002/2017JB014168.
Witte, J. C., and Coauthors, 2017: First reprocessing of Southern Hemisphere Additional Ozonesondes (SHADOZ) profile records (1998–2015): 1. Methodology and evaluation. *J. Geophys. Res.*, **122**, 6611–6636, https://doi.org/10.1002/2016JD026403.
——, A. M. Thompson, H. G. J. Smit, H. Vömel, F. Posny, and R. Stübi, 2018: First reprocessing of Southern Hemisphere Additional Ozonesondes (SHADOZ) profile records: 3. Uncertainty in ozone profile and total column. *J. Geophys. Res. Atmos.*, **123**, 3243–3268, https://doi.org/10.1002/2017JD027791.